Dosimetry of ^{131}I-Labeled 81C6 Monoclonal Antibody Administered into Surgically Created Resection Cavities in Patients with Malignant Brain Tumors

Gamal Akabani, Craig J. Reist, Ilkcan Cokgor, Allan H. Friedman, Henry S. Friedman, R. Edward Coleman, Xiao-Guang Zhao, Darell D. Bigner and Michael R. Zalutsky

Departments of Radiology, Pathology, Medicine and Surgery, Duke University Medical Center, Durham, North Carolina

The objective of this study was to perform the dosimetry of ^{131}I-labeled 81C6 monoclonal antibody (MAb) in patients with recurrent malignant brain tumors, treated by direct injections of MAb into surgically created resection cavities (SCRCs). **Methods:** Absorbed dose estimates were performed for nine patients. Dosimetry was performed retrospectively using probe counts (during patient isolation) and whole-body and SPECT images thereafter. Absorbed doses were calculated for the SCRC interface and for regions of interest (ROIs) 1 and 2 cm thick, measured from the margins of cavity interface. Also, mean absorbed doses were calculated for normal brain, liver, spleen, thyroid gland, stomach, bone marrow and whole body. The average residence time for the SCRC was 111 h (65–200h). **Results:** The average absorbed dose per unit injected activity (range) to the SCRC interface and ROIs 1 and 2 cm thick from the cavity interface were 31.9 (7.8–84.2), 1.9 (0.7–3.6) and 1.0 (0.4–1.8) cGy/MBq, respectively. Average absorbed doses per unit administered activity to brain, liver, spleen, thyroid, stomach, bone marrow and whole body were 0.18, 0.03, 0.08, 0.05, 0.02, 0.02 and 0.01 cGy/MBq, respectively. The high absorbed dose delivered to the SCRC interface may have produced an increase in cavity volume independent of tumor progression. **Conclusion:** At the maximum tolerated dose of 3700 MBq ^{131}I-labeled 81C6 MAb, the absorbed doses to the SCRC interface and ROIs of 1 and 2 cm thickness were estimated to be 1180, 71 and 39 Gy, respectively. The estimated average absorbed dose to the brain was 6.5 Gy. There was no neurological toxicity and minimal hematologic toxicity at this maximum tolerated administration level.

Key Words: radioimmunotherapy; brain tumors; dosimetry

J Nucl Med 1999; 40:631–638

Glioblastoma multiforme (GBM) is the most common primary brain tumor in the adult, and it represents the major primary cause of morbidity and mortality in neuro-oncological practice. Surgery followed by external beam irradiation and chemotherapy is the standard of care for GBM and anaplastic astrocytoma. Surgical resection provides short-term benefit, but it is almost impossible to remove every microscopic trace of the disease, because of the infiltrative characteristic of these brain tumors (*1*). Furthermore, tumor debulking can modify the kinetics of residual cells located at and near the interface of the tumor and normal brain tissue. Tumor debulking may prompt the entry of noncycling residual tumor cells into active division and increase their sensitivity to chemotherapy and radiation treatments (*2*). In addition, a study from the Brain Tumor Cooperative Group showed that preoperative tumor volume was unrelated to survival; however, residual tumor volume immediately after surgery correlates strongly with survival (*3*).

External beam radiation therapy is considered the most effective adjuvant therapy after surgery. The benefit of postoperative radiation therapy has been well established (*4–6*). The median survival of newly diagnosed patients receiving surgery alone was 14 wk in comparison to 35 wk for those undergoing surgery and radiation therapy. However, in conventional radiotherapy, absorbed doses are limited by concerns about normal tissue toxicity, including delayed brain-tissue radionecrosis.

Radioimmunotherapy can also be used as an adjuvant treatment where monoclonal antibodies (MAbs) reactive with tumor-associated antigens are used to deliver radionuclides to tumor cells. The low tumor accumulation of systemically-injected radiolabeled MAbs and the high interstitial pressure in brain tumors are problems that might be circumvented if treatment were performed by local administration (*7–9*). The advantages of a direct administration include bypassing the blood-brain barrier, obtaining high local activity concentration and reducing systemic toxicity. Consequently, in the case of intracystic administration, a highly localized dose can be delivered to residual tumor located at and near the cavity interface. In contrast to external beam radiotherapy, there should be limited damage

to normal brain, because of the short range of β particles, thus reducing the long-term risk for radionecrosis.

This localized therapy approach has been used intratumorally in preliminary studies by Riva et al. (*10*) in which patients underwent multiple injections of ^{131}I-labeled BC-2, with cumulative absorbed doses to the cavity interface between 70 and 410 Gy. Similarly, Hopkins et al. (*11*) assessed absorbed doses to the cavity interface as a function of mean cavity radii and antibody-binding fraction for ^{90}Y-labeled ERIC-1; a range of doses between 20 and 5000 Gy was calculated. The intrathecal administration of ^{131}I-labeled Mel-14, HMFG1, M340 and ^{131}I-labeled 81C6 also have been described elsewhere (*12,13*).

In this article, we present the dosimetry results of a phase I clinical trial using intracystically administered ^{131}I-labeled 81C6 MAb to treat patients with recurrent malignant brain tumors who had received prior external beam therapy. The emphasis of this study is on the dosimetry of the surgically created resection cavities (SCRCs) interface, normal brain and organs, and analysis of the SCRC volume increase determined by subsequent radiographic evidence. A detailed clinical description of this phase I clinical trial has been presented elsewhere (*14*).

MATERIALS AND METHODS

Patient Eligibility

This phase I study was approved by the Duke University Institutional Review Board under Protocol No. 307–97–2R4 and under the Food and Drug Administration Investigational New Drug Permit BB-IND-2692. Patients were required to be eligible for surgical resection and to have a corroborated histologic diagnosis of a recurrent primary or metastatic malignant tumor. Documentation of 81C6 reactivity with tumor biopsy samples was required by immunohistochemistry of either fresh or paraffin-embedded tumor biopsy with 81C6 or affinity-purified polyclonal rabbit antitenascin serum. All patients were tested for circulating antibodies to murine 81C6 IgG$_{2b}$ (human antimouse antibody) as described elsewhere (*15*). After the tumor was resected, an Ommaya or Rickham reservoir and catheter were placed into the SCRC. A Gd-enhanced MRI scan was obtained after craniotomy to assess residual tumor, and rim enhancement could not be measured more than 1 cm beyond the margins of the SCRC.

Only patients with intact resection cavities were eligible for treatment. Patients with subgaleal leakage from the SCRC or with a resection cavity that communicated with the subarachnoid space were not eligible. Informed consent was obtained before therapy.

Antibody Production and Radiolabeling

The monoclonal antibody 81C6 is a murine IgG$_{2b}$ MAb that binds to tenascin, a tumor-associated extracellular matrix glycoprotein present in human gliomas but not in the normal brain. This glycoprotein is also found in melanomas and in breast, lung and squamous cell carcinomas (*16*). The 81C6 MAb was produced in the ascites fluid of athymic mice and purified by passage over a Sepharose-staphylococcal protein-A column, followed by polyethyleneimine ion exchange chromatography. Radiolabeling of 81C6 MAb with ^{131}I was performed by a modified Iodo-Gen procedure (*7*). All preparations had immunoreactivity of more than 50% (*17*), with more than 95% of the radioactivity eluting as IgG on high-

pressure liquid chromatography, and more than 95% precipitating with trichloroacetic acid.

Patient Treatment

Treatment consisted of a single injection of ^{131}I-labeled 81C6 MAb into the patient's reservoir. Each patient was taken to a fluoroscopy suite, where the reservoir was accessed with a butterfly needle under sterile conditions. Between 5 and 10 mL cystic fluid was removed. Approximately 1 mL iopamidol was injected into the reservoir to document the free flow of contrast media out of the distal tip of the reservoir. The patient was then taken to a lead-lined isolation room, where ^{131}I-labeled 81C6 MAb was injected into the reservoir and flushed with 2 mL cystic fluid so that the reservoir was left with minimal residual activity. Patients were placed in isolation until whole-body retention of ^{131}I was less than 1110 MBq (30 mCi), as determined by external measurements using an exposure rate meter. Eligible patients were treated orally with a saturated solution of potassium iodide and 50 μg liothyronine sodium daily, beginning at least 48 h before therapy and continuing for 28 d to decrease [^{131}I]-iodide thyroid uptake.

Patients were treated on a dose-escalation protocol to determine the maximum tolerated dose (MTD). The initial administered activity was 740 MBq (20 mCi) [131]I on 10 mg 81C6. The ^{131}I activity was escalated in 740-MBq (20-mCi) increments on a fixed amount (10 mg) of 81C6 in cohorts of three to six patients per dose level. For doses of 3700 MBq (100 mCi) or more, 20 mg 81C6 MAb was used to avoid radiolysis of these preparations. The patients included in this dosimetry study received administered activities between 2220 and 4440 MBq.

Dosimetry

Because of scheduling restrictions and requirements that patients be able to undergo imaging weekly for 4 wk, absorbed-dose estimates were performed on nine patients only. In these patients, the activity distribution of ^{131}I-labeled 81C6 in the SCRC, normal organs and whole body was assessed. During patient isolation, an exposure-rate meter was used to perform measurements for the whole body and the SCRC to assess time-activity clearance curves. Whole-body and SCRC measurements were obtained at a distance of 1 m from the patient's abdomen and at near-skin contact at the site of intracranial injection, respectively.

Planar whole-body images and SPECT of the head and abdomen were acquired immediately after the patient was discharged from isolation (between 3 and 7 d after MAb injection) and on a weekly basis for a period of 4 wk. All images were acquired on a dual-head gamma camera system equipped with high-energy collimators. An energy window of 15%, centered on the photopeak of ^{131}I, was used in all planar and tomographic image acquisitions. SPECT acquisitions were performed in 360° orbits, and images were acquired in 3° intervals at 20 s per view. These projection data were acquired in 128 × 128 matrices. Standard quantitative SPECT methods were used to determine activity distributions of ^{131}I in the SCRC and in normal organs that accumulated ^{131}I activity (*18–21*). These organs were liver, spleen, stomach and thyroid gland. The analysis of whole-body images was performed using gamma camera system computer software to generate regions of interest (ROIs). This analysis yielded relative clearance curves for the SCRC, normal organs and whole body. Also, blood samples were obtained at approximately 1, 2, 4, 8, 12, 24, 72, 120 and 360 h after ^{131}I-labeled 81C6 administration to measure the activity concentration in blood as a function of time. A trichloroacetic acid (TCA) precipitation

assay was used to assess the protein-associated fraction of ^{131}I in these blood samples.

Whole-Body Dosimetry

Because a fraction of the total administered activity remained in the SCRC, the absorbed dose to the whole body (WB) was calculated based on activity located in the SCRC and activity distributed in the whole body. A serial two-compartmental system was used to model the pharmacokinetics of ^{131}I-labeled 81C6, where the SCRC and the whole body (not including the SCRC) were assumed to be the first and second compartments, respectively. Assuming a monoexponential clearance for the SCRC and whole body, the functional solution for the SCRC activity can be expressed as:

$$A_{SCRC} = A_0 e^{-(\lambda_p + \lambda_{SCRC})t},\qquad \text{Eq. 1}$$

and that for the whole-body activity as:

$$A_{WB} = A_0 \frac{\lambda_{SCRC}}{\lambda_{WB} - \lambda_{SCRC}} (e^{-\lambda_{SCRC}t} - e^{-\lambda_{WB}t})e^{-\lambda_p t},\qquad \text{Eq. 2}$$

where λ represents the effective decay constant for each respective compartment. Probe measurements obtained during patient's isolation at a distance of 1 m from the abdomen and near skin contact at the site of injection provided the fractional activity remaining in the whole body and SCRC ($A_{SCRC} + A_{WB}$) and SCRC (A_{SCRC}), respectively. After a patient's discharge from isolation, whole-body images were used to assess the long-term retention of activity in the SCRC and whole body. Data from probe measurements and whole-body images were normalized to the initial administered activity. Therefore, the whole-body dose was calculated as

$$D_{WB} = \tilde{A}_{WB}S(WB \leftarrow WB) + \tilde{A}_{SCRC}S(WB \leftarrow SCRC).\qquad \text{Eq. 3}$$

S-values for S(WB ← WB) and S(WB ← SCRC) were based on whole-body weight and were calculated using Monte Carlo transport. Figure 1 presents the time-activity data and fitted curves for the SCRC and whole body for patient 6.

Normal Organ Dosimetry

The self-absorbed dose for liver, spleen, stomach and thyroid gland were calculated based on standard quantitative SPECT methods for ^{131}I (18–21). Similarly, based on the adult MIRD phantom and photon Monte Carlo transport, the absorbed dose contribution to these organs from the SCRC was also considered. The estimated S-values for liver, spleen, stomach and thyroid were approximately 1.8×10^{-6}, 1.8×10^{-6}, 1.1×10^{-6} and 1.6×10^{-4} (cGy/MBq-h), respectively. However, the absorbed doses from sources located in the SCRC to the liver, spleen and stomach were neglected, because they were relatively small in comparison to the self-absorbed dose in these organs.

Bone Marrow Dosimetry

Radiation absorbed-dose estimates for bone marrow were also based on the activity in whole blood as a function of time after administration. The activity concentration of ^{131}I in blood samples was measured in a calibrated well scintillation counter. Sgouros (22) has established that absorbed dose estimates for red marrow based on activity in blood samples require a reduction factor to account for the difference in activity in blood and marrow. It has been suggested that the appropriate factor lies between 0.2 and 0.4 (22–24). Here we assume a reduction factor of 0.3. The dose
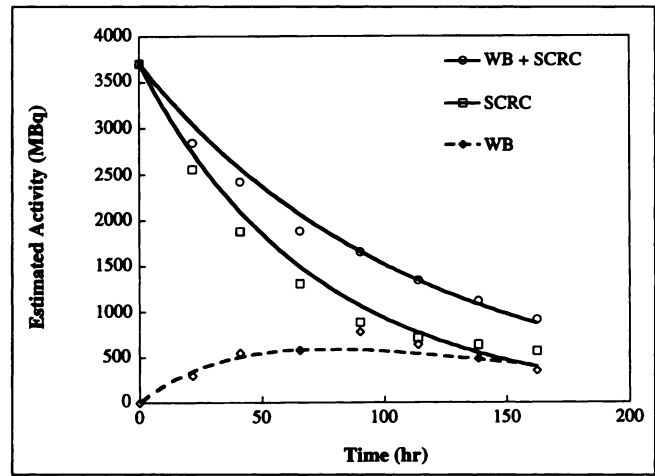

FIGURE 1. Estimated time-activity clearance for whole body (WB) and SCRC for initial administered activity of 3700 MBq (100 mCi) obtained from probe counts from patient 6. Difference between WB + SCRC and SCRC activities represents net activity in whole body. As expected, time-activity clearance for WB follows functional form of serial two-compartment model. This is corroborated from blood sample data obtained after ^{131}I-labeled 81C6 administration.

contribution from the SCRC to bone marrow was also calculated by means of photon Monte Carlo transport. The estimated S-value for bone marrow was 8×10^{-5} (cGy/MBq-h).

SCRC and Normal Brain Dosimetry

Knowledge of the range of absorbed doses as a function of depth from the SCRC interface and in normal brain tissue is of importance in gaining an understanding of radiographic analysis, normal tissue toxicity (radionecrosis) and tumor control during treatment with ^{131}I-labeled 81C6 MAb. Gd-enhanced T_1-weighted axial MR images of each patient's head were obtained immediately after surgery. Using these images, a three-dimensional reconstruction of the head and SCRC was generated, and the volume of the SCRC was calculated using current image analysis software (VoxelView 2.5.4; Vital Images, St. Paul, MN). This volume was then used to estimate the initial activity concentration in the SCRC at the time of administration, and a uniform activity concentration was assumed. The activity clearance from the SCRC was determined from probe counts before and whole-body images after patient discharge from isolation.

Depth-dose calculations and corresponding isodose curves for the SCRC, SCRC interface and normal brain were then performed using the three-dimensional discrete Fourier transform convolution method based on a dose-kernel for ^{131}I. Briefly, this method uses the three-dimensional activity distribution of an organ or region and carries out the convolution with the ^{131}I kernel. As a result, it provides the three-dimensional dose distribution for such organ or region. This method is described in detail elsewhere (25). Isodose curves were generated based on the geometry for each patient, as determined by a three-dimensional reconstruction of MR images. The dose to the whole brain also was calculated based on the contributions from activity within the SCRC and blood in the brain.

Using this methodology, absorbed doses to regions of the brain which are of neurological relevance, such as corpus callosum and the frontal, temporal and parietal lobes, can be calculated. Also, average absorbed doses for normal brain tissues located at 1.0 and

2.0 cm from the SCRC interface and for whole-brain tissue were also calculated for comparison to external beam radiotherapy.

MRI Measurements

The SCRC volume was measured as a function of time to assess changes in SCRC volume. The last available MR images for a patient after progressive disease was diagnosed were used to assess the final SCRC volume. The fractional SCRC increase was defined as the ratio between the final and initial volumes. To perform these analyses, Gd-enhanced T_1-weighted axial MR images of the head (3-mm thick contiguous slices) were obtained on a monthly basis after ^{131}I-labeled 81C6 MAb therapy.

RESULTS

Patient Characteristics

All nine patients in this dosimetry study were diagnosed at the time of therapy with GBM. All patients had undergone prior surgery and had been treated with prior external beam radiotherapy (58–62 Gy total dose) and chemotherapy. Administered doses of ^{131}I-labeled 81C6 for each of these nine patients were as follows: 2 at 2220 MBq (60 mCi)/10 mg, 2 at 2960 MBq (80 mCi)/10 mg, 2 at 3700 MBq (100 mCi)/20mg, and 3 at 4440 MBq (120 mCi)/20 mg. In total, there were 36 treatments in this phase I study. However, initial and follow-up MR images were available for 33 and 25 treatments, respectively.

Clearance Characteristics of ^{131}I-Labeled 81C6 in SCRC and Normal Tissues

The retention in the SCRC and distribution in normal organs of ^{131}I-labeled 81C6 varied considerably among these patients. A large fraction of the total activity remained in the SCRC, and lower activity concentrations were detected in the liver and spleen. Moreover, uptake of ^{131}I activity (presumably as free iodine) was also detected in the thyroid gland and stomach. The time-activity curves for the SCRC and normal tissues, generated from the relative probe counts and serial gamma camera views, were described by either monoexponetial or biexponential functions (Fig. 2A).

As expected, the time-activity clearance for whole body excluding the SCRC activity follows the functional form of a serial two-compartment model. Table 1 provides a summary of effective half-lives for the group of nine patients. In this table, T_α and T_β denote the effective half-lives for the α

and β phases, respectively, and the ratio between the α and β coefficients (α/β). The activity in blood was characterized by an exponential uptake phase followed by an exponential clearance phase (Fig. 2B). TCA assay in blood samples showed that more than 60% of the ^{131}I activity remained bound to 81C6 protein during the first 24 h after administration, and this increased up to 95% afterwards. Long-term retention (T_β) was observed in the SCRC, thyroid and liver, where effective half-lives approached the physical half-life for [131]I. The average effective half-lives T_α and T_β of ^{131}I-labeled 81C6 in the SCRC were 79 and 167 h, respectively. Patients remained in isolation for a period of 3–7 d, depending on whole-body clearance rate.

Radiation Absorbed Dose Estimates

Table 2 summarizes the administered activities of ^{131}I-labeled 81C6, measured SCRC volumes and absorbed dose estimates for the SCRC interface, for ROIs 1 and 2 cm thick from the SCRC interface, and for thyroid gland, liver, spleen, stomach, bone marrow and whole body for nine patients. The estimated absorbed dose per unit administered activity to the cavity interface varied considerably among all nine patients as a result of cavity volume and SCRC residence time. Based on data obtained from these patients, the average absorbed dose per unit administered activity to the SCRC interface and ROIs 1 and 2 cm thick from the margins of the cavity interface were 31.9 (7.8–84.2), 1.9 (0.7–3.7) and 1.1 (0.4–1.9) cGy/MBq, respectively. However, the absorbed dose to the SCRC interface exceeded 300 Gy in all nine patients. As an example, Figure 3 presents the isodose contours coregistered with a Gd-enhanced T_1-weighted axial MR image for patient 6, who received an administered activity of 3700 MBq (100 mCi).

All dosimetry calculations for thyroid, liver, spleen and stomach were based on image analysis. Absorbed dose estimates for red marrow were based on time-activity measurements of ^{131}I in blood starting immediately after administration. The average absorbed dose per unit administered activities for whole brain, liver, spleen, thyroid, stomach, bone marrow and whole body were 1.8×10^{-1}, 3.1×10^{-2}, 8.0×10^{-2}, 5.1×10^{-2}, 2.2×10^{-2}, 1.5×10^{-2} and 1.1×10^{-2} cGy/MBq, respectively.

The majority of patients undergoing this therapy modality

FIGURE 2. (A) [131]I activity concentration in thyroid, liver and spleen as function of time postinjection. Data points denote whole-body imaging performed immediately after patient's discharge from isolation and 1, 2 and 3 wk afterwards. Quantitative SPECT imaging was used to assess activity concentrations in organs in which imaging was quantifiable. Data were extrapolated to t = 0 to assess total absorbed dose. (B) Measured activity concentration in blood for ^{131}I as function of time after administration of 3700 MBq (100 mCi) ^{131}I-labeled 81C6.
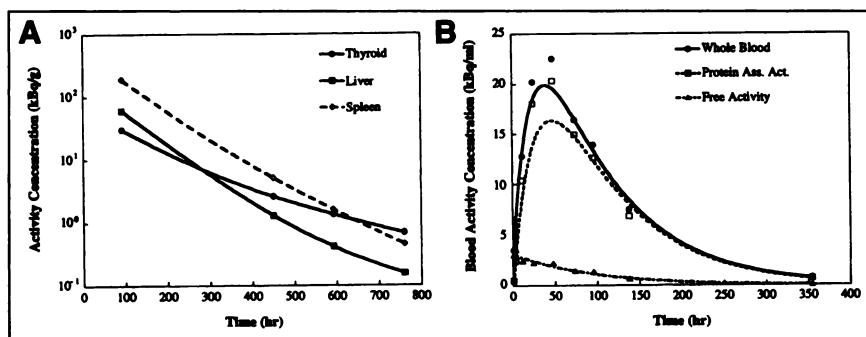
TABLE 1
Effective Half-Life (h) of ^{131}I-Labeled 81C6 in the SCRC and Normal Organs

Patient	SCRC T_α	SCRC T_β	SCRC (α/β)	Liver T_α	Liver T_β	Liver α/β	Spleen T_α	Spleen T_β	Spleen α/β	Thyroid T_α	Thyroid T_β	Thyroid α/β	Stomach T_α	Stomach T_β	Stomach α/β	Blood T_α	Blood T_β	Blood α/β
1	88	164	80	40	160	32	120	—	—	40	199	15	50	102	22	12	70	−1.0
2	59	160	5	42	142	25	84	126	65	37	168	45	39	83	61	69	70	−1.0
3	64	155	50	43	152	58	90	—	—	NA*	—	—	50	104	53	11	65	−1.0
4	59	177	200	42	155	84	31	118	70	45	163	21	54	87	126	53	54	−1.0
5	83	173	19	58	173	60	56	104	7.5	70	197	6.5	NA*	—	—	35	109	−1.0
6	45	170	100	53	141	78	62	91	86.4	39	205	12	45	120	64	51	52	−1.0
7	89	172	60	33	185	63	56	117	34.9	67	174	4.5	47	93	75	49	101	−1.0
8	44	176	124	42	143	75	75	95	78.7	60	185	18	40	89	90	24	52	−1.0
9	140	—	—	115	—	—	95	—	—	166	167	−1	NA*	—	—	55	61	−1.0

*Organ uptake too low for activity quantitation by noninvasive imaging.

SCRC = surgically created resection cavities; T_α = effective half-life for α phase; T_β = effective half-life for β phase; α/β = ratio between α and β coefficient.

are not able to bear further imaging studies because of clinical status or scheduling restrictions. Therefore, absorbed dose estimates to the SCRC interface and margins must be based exclusively on data obtained before and during patient isolation. A simplified model based on SCRC volume and residence time was developed to assess gross absorbed doses to the SCRC interface and cavity margins. However, this gross model was unable to provide absorbed dose estimates for regions of the brain of neurological relevance. This simplified model represented the SCRC as a sphere, where absorbed doses were calculated as a function of SCRC volume. The SCRC volume can be obtained from Gd-enhanced T_1-weighted axial MR images made immediately after surgery. The absorbed dose to the cavity interface and other ROIs then can be expressed using an S-value.

Therefore, the dose to the SCRC interface and ROIs beyond the cavity margins can be expressed as

$$D_{ROI} = A_{SCRC} S(ROI \leftarrow SCRC) \tau_{SCRC}, \qquad Eq. 4$$

where D_{ROI} is the absorbed dose to a given ROI (cavity interface and ROIs of 1 and 2 cm thick from the cavity margins), A_{SCRC} is the administered activity into the SCRC, $S(ROI \leftarrow SCRC)$ is the corresponding S-value for a given ROI, and τ_{SCRC} is the estimated residence time in the SCRC. A gross estimate of the residence time τ_{SCRC} can be obtained from head-probe measurements normalized to the initial administered activity. In this manner, gross estimates can be obtained from future patients who cannot undergo additional radionuclide imaging.

TABLE 2
Administered Activities of ^{131}I-Labeled 81C6, Whole-Body Weights, Estimated SCRC Volumes and Corresponding Radiation Absorbed-Dose Estimates to the SCRC and Normal Organs

Patient no.	Administered activity (MAb) MBq	Administered activity (MAb) (mg)	WB weight (kg)	SCRC volume (cm³)	SCRC residence time* (h)	SCRC† Interface	SCRC† (1 cm)	SCRC† (2 cm)	Brain	Liver	Spleen	Thyroid	Stomach	Bone marrow	Whole body
1	2,220	(10)	99	8.9	128	187,000	8,200	4,100	460	130	216	224	87	34	22
2	2,220	(10)	68	39.0	87	30,000	2,400	1,400	400	130	188	103	80	35	26
3	2,960	(10)	77	35.5	94	48,000	3,700	2,200	450	98	332	105	23	37	30
4	2,960	(10)	83	18.0	111	109,000	6,300	3,500	410	67	300	178	41	39	30
5	3,700	(20)	83	13.8	121	193,000	10,100	5,400	730	175	559	184	120	56	42
6	3,700	(20)	75	51.2	66	29,000	2,600	1,600	400	38	145	145	32	58	41
7	4,440	(20)	49	34.3	130	103,000	7,800	4,700	940	42	303	103	105	64	56
8	4,440	(20)	91	38.6	65	46,000	3,600	2,200	470	69	157	155	65	41	38
9	4,440	(20)	87	28.4	200	190,000	13,500	7,800	1,470	99	125	300	85	86	60
Average absorbed dose per unit administered activity (cGy/MBq)						31.90	1.91	1.07	0.181	0.031	0.080	0.051	0.022	0.015	0.011

*Estimated residence time from probe counts, quantitative SPECT and whole-body imaging.
†Estimated absorbed doses at the SCRC interface 1 and 2 cm from the margins of SCRC interface.
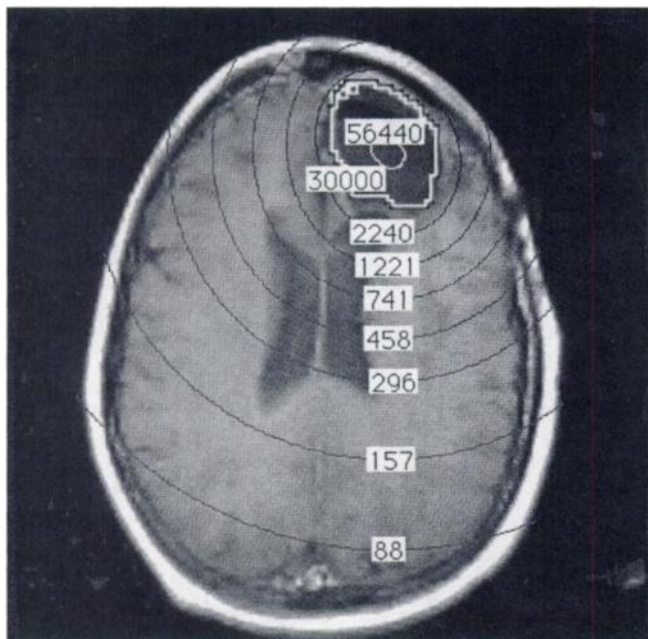WB = whole body; SCRC = surgically created resection cavity.

FIGURE 3. Gadolinium-enhanced T₁-weighted axial MR image with coregistration of isodose contours for patient 6, who received administered dose of 3700 MBq (100 mCi). Approximate cavity volume was 51.2 cm³ and absorbed doses near center of cavity and cavity interface were calculated at 56,440 and 30,000 cGy, respectively. Average absorbed dose over 1- and 2-cm thick regions from margins of cavity interface were estimated at 2700 and 1700 cGy, respectively. Estimated average absorbed dose to normal brain tissue was 400 cGy.

SCRC Volumes

The initial SCRC volumes among patients varied considerably on the basis of tumor location and extent. The average initial cavity volume among all evaluable patients was 20 cm³ (n = 33, range 0.5–60 cm³), where the volume of the Ommaya or Rickham reservoir was not included in these measurements. The SCRC volume and enhancing rim were also measured as a function of time in 25 evaluable patients. The estimated average increase in cavity volume was 2.4.

DISCUSSION

The goal of this radioimmunotherapy treatment approach with ¹³¹I-labeled 81C6 MAb administered into SCRCs for malignant brain tumors is to deliver a highly localized absorbed dose to the margins of the SCRC where residual tumor is located. However, such tumor extent varies from several millimeters to a few centimeters within normal brain tissue (*1,26*). The methods presented here established the necessary volumetric information and activity distribution needed to assess absorbed doses to the SCRC interface and normal brain tissue. Furthermore, isodose contours were generated to correlate absorbed doses to specific regions of the brain with future radiographic changes that might result from brain-tissue radionecrosis or tumor progression. This correlation is of relevance and requires further study.

The pharmacokinetics and dosimetry results for the SCRC obtained in this study are similar to those reported by Papanastassiou et al. (*12*) using ¹³¹I-labeled ERIC-1 MAb, where the radiolabel remained mainly in the SCRC with limited leakage into the systemic blood pool. They reported an average dose for the whole body, bone marrow and whole brain of 1.1×10^{-2}, 1.4×10^{-2} and 0.28 cGy/MBq, respectively. Also, absorbed doses to tumor were expressed as a function of percentage binding and were estimated to be between 4 and 119 cGy/MBq. In this study we obtained equivalent absorbed doses per unit administered activity for the whole body and bone marrow. However, we obtained a lower absorbed dose per unit administered activity for the whole brain (0.18 cGy/MBq). This was probably due to the fact that our calculations were performed on a cavity-specific basis, taking into consideration the shape, size and location of the SCRC within the brain, rather than using a single S-value for all patients. A large fraction of the initial administered activity remained in the SCRC; thus absorbed doses to the SCRC interface and 1 and 2 cm from the margins of the cavity interface were 31.9 (7.8–84.2), 1.9 (0.7–3.7) and 1.1 (0.4–1.9) cGy/MBq, respectively. These calculations were based on the three-dimensional convolution method using the ¹³¹I kernel, and isodose contours were calculated and superimposed over MR images of the head obtained before therapy.

Overall, TCA analysis in blood samples showed that more than 95% of ¹³¹I activity remained bound to protein and only a small fraction (< 5%) of the total activity was present as free iodine. This effect is clearly seen in the long-term retention of ¹³¹I-labeled 81C6 MAb in the SCRC, where T_β approximated the physical half-life of ¹³¹I (Table 1). Papanastassiou et al. (*12*) also observed an increase in the SCRC residence-time as a function of administered protein dose. In this study, however, we did not observe a statistically significant increase in the SCRC residence time in those patients who were treated with a 20-mg protein dose of 81C6. The average SCRC residence time for those patients treated at the 10- and 20-mg dose level was 101 ± 23 h and 132 ± 67 h, respectively.

The MTD for this phase I study was 3700 MBq (100 mCi) ¹³¹I-labeled 81C6 (20 mg), and neurotoxicity was the dose-limiting factor (*14*). At this administration level, the estimated absorbed dose to the SCRC interface was approximately 1180 (290–3200) Gy, and the estimated average absorbed doses to ROIs 1 and 2 cm thick from the margins of the cavity interface were 71 (26–136) and 40 (16–68) Gy, respectively. The average absorbed doses to the brain, liver, spleen, thyroid, stomach, bone marrow and whole body were estimated at 670, 114, 295, 188, 80, 54 and 41 cGy, respectively.

All patients received prior external beam therapy; thus, delayed cerebral radionecrosis represented a significant risk. Significant clinical neurotoxicity developed a few months after treatment in three patients treated at the 4440-MBq

(120-mCi) administration level. Based on Table 2, the average absorbed dose to normal brain tissue was approximately 8 Gy. These patients received a total absorbed dose to normal brain tissue from external beam radiotherapy of approximately 60–62 Gy. Therefore, the overall cumulative absorbed dose, including that received from ^{131}I-labeled 81C6 MAb, was estimated at 68–70 Gy, which clearly exceeds the dose limits established for brain tissue neurotoxicity (4,27). However, the risk for delayed tissue radionecrosis for this localized treatment modality should be lower than that for interstitial brachytherapy in recurrent patients. Indeed, none of the patients treated in this phase I study required reoperation for treatment for radionecrosis. In contrast, approximately 64% of the patients treated with brachytherapy require reoperation for symptomatic radionecrosis within 12 mo after treatment (28,29). It is important to notice the fast decrease in absorbed dose as a function of depth from the margins of the cavity interface (Fig. 3). This extremely high dose delivered to the margins of SCRC may have produced early radionecrosis over a thin layer of brain tissue which may, in turn, have eroded and led to an increase in cavity volume independent of tumor progression. This increase in cavity volume was observed in 15 of 25 patients analyzed, where the estimated average cavity increase was 2.4 with a range between 0.96 and 5.6.

Based on the clinical reports, there was no hematological or neurological toxicity observed in those patients treated at or below the 2960-MBq (80-mCi) administration level. However, two Grade IV intravenous major hematological toxicities occurred at the 3700 and 4440 MBq administration levels, where the estimated absorbed dose to bone marrow was 54 and 86 cGy (patient 9), respectively. In contrast with systemic radioimmunotherapy, myelotoxicity generally is the dose-limiting factor where absorbed doses to red marrow can be as high as 600 cGy (30,31). This localized therapy delivered absorbed doses to red marrow approximately 10 to 20 times lower given the same administered activity. Thus, the low absorbed doses to normal organs, bone marrow and whole body of this therapy modality are a benefit.

Only 9 of 36 treatments were used for this dosimetric study; in future studies not all patients will be able to undergo radionuclide imaging. Therefore, it is necessary to assess gross dose estimates to the SCRC interface and normal brain tissue based on predetermined S-values as a function of SCRC volume and estimated residence time. Based on a simplified model in which the SCRC was assumed to a be a sphere, S-values for the SCRC interface and ROIs 1 and 2 cm thick from the margins of the cavity interface were presented as a function of cavity volume. The SCRC volume can be calculated from MR images obtained immediately after craniotomy, and the SCRC residence time can be assessed from head and whole-body probe counts. However, these dose estimates should be used only for future reference and for comparison with other therapy modalities, such as external beam therapy.

CONCLUSION

Treatment of previously irradiated patients who have recurrent primary or metastatic brain tumors with ^{131}I-labeled 81C6 MAb administered into the SCRC is well tolerated at the MTD level of 3700 MBq. At the maximum tolerated administered activity, an estimated dose between 290 and 3200 Gy was delivered to the resection cavity interface. At this level, the absorbed doses to ROIs 1 and 2 cm from the margins of the cavity interface were between 26 and 137, and 16 and 68, respectively. The estimated absorbed doses to whole brain, liver, spleen, thyroid, stomach, bone marrow and whole body were 6.7, 1.1, 2.9, 1.8, 0.8, 0.5 and 0.4 Gy, respectively. It is hoped that this dosimetry data will facilitate the interpretation of clinical studies with localized-regional administration of ^{131}I-labeled 81C6 MAb and lead to improvements in the treatment of brain tumors using labeled MAbs.

REFERENCES

1. Burger PC, Heinz ER, Shibata T, Kleihues P. Topographic anatomy and CT correlations in the untreated glioblastoma multiforme. *J Neurosurg.* 1988;68:698–704.
2. Hoshino T. A commentary on the biology and growth kinetics of low grade and high grade gliomas. *J Neurosurg.* 1984;61:895–900.
3. Wood JR, Green SB, Shapiro WR. The prognostic importance of tumor size in malignant gliomas: a computed tomographic scan study by the Brain Tumor Cooperative Group. *J Clin Oncol.* 1988;6:338–343.
4. Walker MD, Alexander E, Hunt WE, et al. Evaluation of BCNU and/or radiotherapy in the treatment of anaplastic gliomas. A cooperative clinical trial. *J Neurosurg.* 1978;49:333–343.
5. Sheline GE. Radiotherapy for high grade gliomas. *Int J Radiat Oncol Biol Phys.* 1990;18:793–803.
6. Davies E, Clarke C, Hopkins A. Malignant cerebral glioma--I: Survival, disability, and morbidity after radiotherapy. *Br Med J.* 1996;313:1507–1512.
7. Zalutsky MR, Moseley RP, Coakham HB, et al. Pharmacokinetics and tumor localization of ^{131}I-labeled anti-tenascin monoclonal antibody 81C6 in patients with gliomas and other intracranial malignancies. *Cancer Res.* 1989;49:2807–2813.
8. Kemshead JT, Papanastassiou V, Coakham HB, et al. Monoclonal antibodies in the treatment of central nervous system malignancies. *Eur J Cancer.* 1992;28:511–513.
9. Jain RK, Baxter LT. Mechanisms of heterogeneous distribution of monoclonal antibodies and other macromolecules in tumors: significance of elevated interstitial pressure. *Cancer Res.* 1988;48:7022–7032.
10. Riva P, Arista A, Tison V, et al. Intralesional radioimmunotherapy of malignant gliomas: an effective treatment in recurrent tumors. *Cancer.* 1994;73:1076–1082.
11. Hopkins K, Chandler C, Bullimore J, et al. A pilot study of the treatment of patients with recurrent malignant gliomas with intratumoral yttrium-90 radioimmunoconjugates. *Radiother Oncol.* 1995;34:121–131.
12. Papanastassiou V, Pizer BL, Coakham HB, et al. Treatment of recurrent and cystic malignant gliomas by a single intracavity injection of ^{131}I monoclonal antibody: feasibility, pharmacokinetics and dosimetry. *Br J Cancer.* 1993;67:144–151.
13. Brown MT, Coleman RE, Friedman AH, et al. Intrathecal ^{131}I-labeled antitenascin monoclonal antibody 81C6 treatment of patients with leptomeningeal neoplasms

or primary brain tumor resection cavities with subarachnoid communication: phase I trial results. *Clin Cancer Res.* 1996;2:963–972.

14. Bigner DD, Brown MT, Friedman AH, et al. Iodine-131-labeled anti-tenascin monoclonal antibody 81C6 treatment of patients with recurrent malignant gliomas: phase I trial results. *J Clin Oncol.* 1998;16:2202–2212.

15. Courtenay-Luck NS, Epenetos AA, Moore R, et al. Development of primary and secondary immune responses to mouse monoclonal antibodies used in the diagnosis and therapy of malignant neoplasms. *Cancer Res.* 1986;46:6489–6493.

16. Bourdon MA, Wikstrand CJ, Furthmayr H, et al. Human glioma-mesenchymal extracellular matrix antigen defined by monoclonal antibody. *Cancer Res.* 1983;43:2796–2805.

17. Lindmo T, Boven E, Cuttitta F, et al. Determination of the immunoreactive fraction of radiolabeled monoclonal antibodies by linear extrapolation to binding at infinite antigen excess. *J Immunol Methods.* 1984;72:77–89.

18. Leichner PK, Koral KF, Jaszczak RJ, et al. An overview of imaging techniques and physical aspects of treatment planning in radioimmunotherapy. *Med Phys.* 1993;20:569–577.

19. Israel O, Iosilevesky G, Front D, et al. SPECT quantification of I-131 concentration in phantoms and human tumors. *J Nucl Med.* 1990;31:1945–1949.

20. Leichner PK, Akabani G, Colcher D, et al. Patient-specific dosimetry of indium-11- and ytrium-90-labeled monoclonal antibody CC49. *J Nucl Med.* 1997;38:512–516.

21. Smith MF, Gilland DR, Coleman RE, Jaszczak RJ. Quantitative imaging of I-131 distributions in brain tumors with pinhole SPECT: a phantom study. *J Nucl Med.* 1998;39:856–864.

22. Sgouros G. Bone marrow dosimetry for radioimmunotherapy: theoretical considerations. *J Nucl Med.* 1993;34:689–694.

23. Siegel JA, Wessels BW, Watson EE, et al. Bone marrow dosimetry and toxicity for radioimmunotherapy. *Antibody Immunoconj Radiopharm.* 1990;3:213–233.

24. Whitwell JR, Spiers FW. Calculated beta-ray dose factors for trabecular bone. *Phys Med Biol.* 1976;21:16–38.

25. Akabani G, Hawkins WG, Eckblade MB, et al. Patient specific dosimetry based on quantitative SPECT imaging and three-dimensional discrete Fourier transform convolution. *J Nucl Med.* 1997;38:308–314.

26. Halperin EC, Bentel G, Heinz ER, Burger PC. Radiation therapy treatment planning in supratentorial glioblastoma multiforme: an analysis based on post mortem topographic anatomy with CT correlations. *Int J Radiat Oncol Biol Phys.* 1989;17:1347–1350.

27. Vick NA, Paleologos NA. External beam radiotherapy: hard facts and painful realities. *J Neurooncol.* 1995;24:93–95.

28. Leibel SA, Gutin PH, Wara WM, et al. Survival and quality of life after interstitial implantation of removable high-activity iodine-125 sources for the treatment of patients with recurrent malignant gliomas. *Int J Radiat Oncol Biol Phys.* 1989;17:1129–1139.

29. Wen PY, Alexander E III, Black PM, et al. Long-term results of stereotactic brachytherapy used in the initial treatment of patients with glioblastomas. *Cancer.* 1994;73:3029–3036.

30. Behr TM, Sharkey RM, Juweid ME, et al. Phase I/II clinical radioimmunotherapy with an iodine-131-labeled anti-carcinoembryonic antigen murine monoclonal antibody IgG. *J Nucl Med.* 1997;38:858–870.

31. Tempero M, Leichner P, Dalrymple G, et al. High-dose therapy with iodine-131-labeled monoclonal antibody CC49 in patients with gastrointestinal cancers: a phase I trial. *J Clin Oncol.* 1997;15:1518–1528.